Effect of Slope on the Stability of Riverbanks with a Mobile Bed: An Experimental Study

Mohammad Jamea[1], Mohsen Solimani Babarsad[2*], Mohammad Hosein Poormohammadi[3],

Hosein Ghorbanizadeh Kharrazi[4]

1,3- Department of Civil Engineering, Water Resources Engineering and Management, Shoushtar Branch, Islamic Azad University, Shoushtar, Iran.
2,4- Department of Water Sciences, Water Science and Environmental Research Center, Shoushtar Branch, Islamic Azad University, Shoushtar, Iran.

[*] **Mohsen.solb@gmail.com**

Abstract

The interaction of the flow and riverbank particles might cause riverbank erosion and collapse in the long term. In riverbank areas with deposited fine sediments subjected to the tides and changes in water level, there is a greater possibility of bank collapse, and the establishment of heavyweight protective structures and ripraps makes the bank more unstable. This research aims to study the effects of changing slope on riverbank stability in mobile bed conditions. Accordingly, 21 experiments were conducted on the sediments at different depths with three different gradients (20, 25, and 30 degrees). According to the results, the riverbank with a 20-degree slope was destroyed after the other two slopes (25 and 30 degrees). With Froude numbers over 0.2, all the banks became unstable; however, it takes a longer time for the lower slope, compared to the other slopes, to become unstable. By the increase in the Froude number of paricles Fr_a and the flow depth, the collapse time T_f also decreased, which can be explained by moving away from the incipient motion of the bed and bank particles. In addition, the destruction occurred faster under live bed conditions, compared to clear water conditions.

1. Introduction

Riverbank instability and changes in hydraulic and geometric properties of rivers lead to the river bank and bed erosion, thus reducing the stability of structures along rivers. These problems might have detrimental effects on urban infrastructure, and therefore it is of great importance to examine and protect riverbanks. (Jafarnejad et al., 2018)

Bank stabilization is commonly known to prevent erosion along rivers. Two methods can be used to protect riverbanks against the parallel flow. One is to protect slopes against the attacking agents, and the other is to modify these attacking agents to reduce or remove their destructive effects. Bank protection methods can generally be divided into two groups: 1) indirect protection methods and 2) direct protection methods. An indirect protection method involves measures taken inside the river to reduce the erosive force of the stream, and is realized by sedimentation and keeping the stream away from slopes, such as using breakwaters. A direct protection method, on the other hand, uses the riverbank modifications and places them in the space between the channel side and the stream, so that the risk of erosion can be reduced. Examples are the changing of the riverbank structure and slope. In the following, a review of the previous studies on riverbank protection and stability using direct and indirect methods is provided.

Etminan et al. (2020), Thorne et al. (2020), Hackney et al. (2020), Krzeminska et al. (2019), and Li et al. (2018) tried to examine the performance of structures and flow hydraulics to stabilize and protect riverbanks and waterways based on the laboratory, numerical and field modeling.

Jafarnejad et al. (2019) investigated fixed-bed rivers and concluded that the second layer (filter) can significantly delay the erosion time, while the riprap erosion rate increases. Since the angle of the riprap particles becomes closer to the angle of repose for riprap, the second layer exerts a more stabilizing effect.

Ravindra et al. (2020) examined the riverbank stability with riprap coverage and without toe support to conclude that rockfill dam stability could significantly be increased by strengthening the rockfill dam toe, constructed in tandem with the downstream rockfill shoulder.

Froehlich (2013) separated the gravitational force from the buoyant force acting on a particle to evaluate moments resisting overturning versus moments promoting overturning of a sigle rock particle. Depending on the channel bed, side slope and water slope, the gravitational and buoyant forces can result in the moments of resisting overturning or promoting overturning.

Chu-Agor et al. (2008) experimentally investigated the rate of underground flow and hydraulic parameters affecting internal erosion and concluded that the failure time of the bank depends on the water head and that the slope has less effect on the failure time. They reported similar times for 5% and 10% slopes.

Based on field observations, Wilson et al. (2017) experimentally studied the effects of soil properties on seepage and collapse of slopes. The flow onset time and flow intensity depended linearly on the slope of the enclosing layer. The results confirmed that by the falling of the flood hydrograph, the slope erosion increased in the presence of the delayed subsurface flow or seepage.

Fox et al. (2018) developed an experimental model of sediment transport associated with internal erosion of vertical riverbanks with cohesive material. Accordingly, they described the relationship between sediment flow and seepage flow and formulated a sediment equation based on shear strength in rivers considering seepage force.

Schnellmann et al. (2019) introduced a physical model to show the effects of climate variations on unsaturated soil slopes. They explored the rising and falling of water level in non-saturated slopes using physical and numerical models. The experimental and numerical results were in good agreement regarding the non-saturated soil with complex behavior.

Froehlich (2013) tried to show the effects of slopes on riverbank riprap stability, using "particle angle of initial yield" developed by Grace et al. (1973).

Cancienne et al. (2019) sought to determine the importance of seepage undercutting relative to bank shear strength, bank angle, soil pore-water pressure, and root reinforcement. They formulated two equations for riverbanks with sand and gravel beds to estimate the channel width after erosion.

Bakhtiari et al. (2012) experimentally showed that rotational failure is more probable than shear failure. As the density of soil block increases, the critical depth of scouring

increases, which in turn results in cuntilever failure.

Azinfar et al. (2018) developed a model of single block stability in breakwaters using a safety factor. They assumed that a single block is stable when the forces causing displacement are weaker than the buoyant force.

The effects of mobile bed have been ignored in previous studies. They have mostly focused on rock riprap particles and slopes. The present work aims to examine the influence of slope and flow rate on riverbank stability in the mobile bed conditions based on laboratory modeling. Figure 1 shows an example of riverbank disruption.

Fig. 1 River bank disruption, Padma River, India (Hackney et al., 2020)

2. Materials and method

In this research, the effects of the bank slope and hydraulics on riverbank stability in mobile bed conditions has been investigated. In this context, the related factors and relationships have been defined using dimensional analysis.

2.1. Dimensional analysis

The parameters affecting riverbank stability are shown in Table 1. After extracting these parameters, the dimensionless parameters were also extracted using Buckingham method

Table 1. Effective parameters

Parameter name	Parameter Symbol
Viscosity	μ
Density	ρ
depth of water	h
Flow rate	U
Acceleration of gravity	g
Longitudinal slope	S
Bank slope	α
Channel width	W
Fail time	T_f
Sediment granulation	D_{50}
Specific gravity of blocks = ρ_s/ρ	S_B
Incipient motion velocity	U^*

The variables from Table 1 are given in Relation (1).

$$f = (U, g, S, W, h, \rho, \rho_s, \alpha, T_f, D_{50}, S_B, U^*) \quad (1)$$

Since in all experiments, the shear Reynolds number (Re^*) is above 1250 and hence in the range of turbulent flow, the effect of fluid viscosity can be ignored. To determine the dimensionless numbers affecting the time of failure, dimensional analysis was carried out using Buckingham method, as shown in Relation (2).

$$f = (\frac{U}{\sqrt{(S_B - 1)gh}}, \frac{Uh}{\vartheta}, T_f, \frac{h}{s}, \frac{U}{U^*}, \frac{W}{h}, \frac{h}{D_{50}}) \quad (2)$$

In Eq. (2), $\frac{U}{\sqrt{(S_B-1)gh}}$ the modified Froude number is denoted by Fr_d, α is the bank slope, $\frac{Uh}{\vartheta}$ is the Reynolds number, $t^* = \frac{t_f}{t_{tot}}$ is the failure time, and $th^* = \frac{t_f u^*}{h}$ is the dimensionless ratio of incipient motion velocity. By rewriting Eq. (2), thus:

$$f = \left(Fr_d, T_f, \frac{h}{s}, \frac{U}{U^*} \right) \quad (3)$$

2.2. Physical Model

In these experiments, a closed-system flume of 15 meters long, 90 cm wide and 60 cm high yielding a flow rate of up to 0.08 m³/sec was built at Sediment Research Center of Khuzestan Water and Power Organization, Ahvaz, Iran. Besides, the flow rate was measured at the flume inlet using an electromagnetic flow meter with an accuracy of ±0.02 liters/second. Figure 2 shows the flume specifications and site conditions.
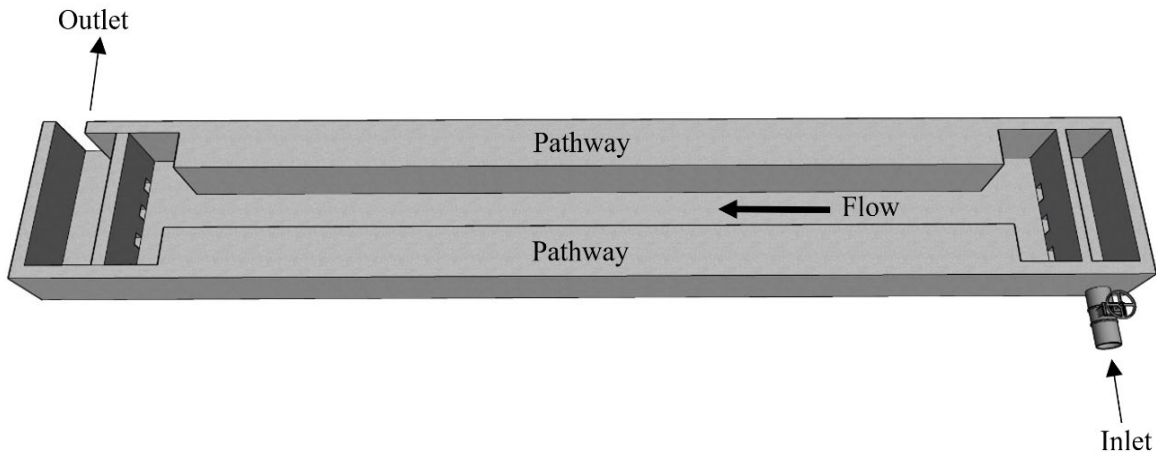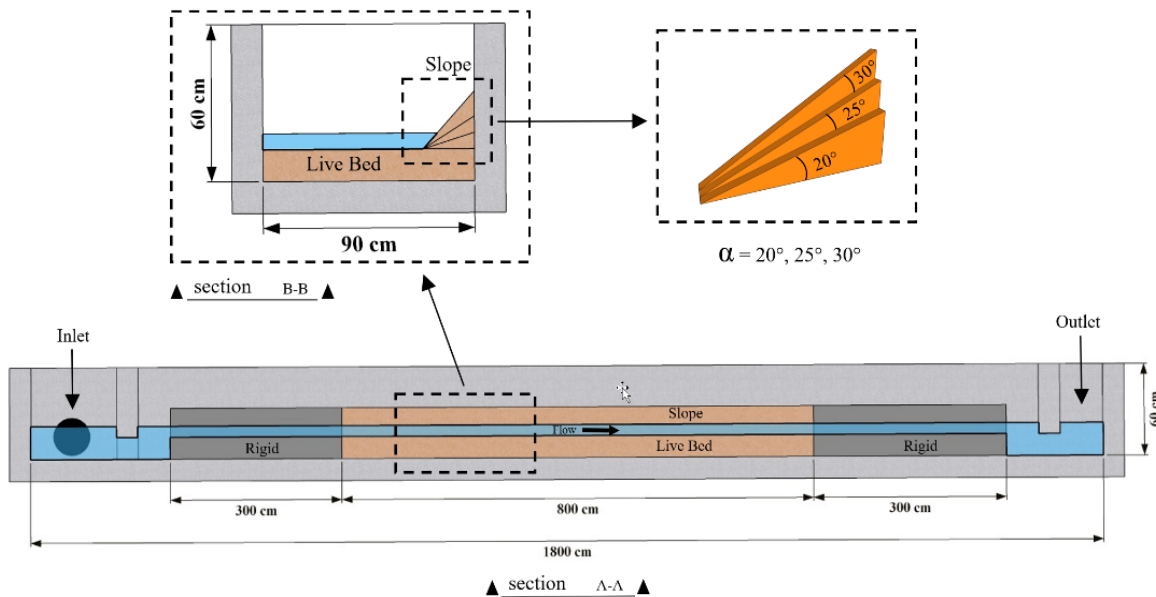

Fig 2. Laboratory flume site-plan

Fig 3. Laboratory flume sections

At the starting and ending 3 meters of the flume, the flume bed and walls were rigid with concrete mortar; however, in the middle part as long as 8 meters, the bed and walls (walls with three different slopes) were filled with river sediments of granular sizes of $D_{50} = 0.2$ and $D_{90} = 0.3$ mm. Table 2 shows the specifications of the conducted experiments.

Table 2. Specifications of experiments

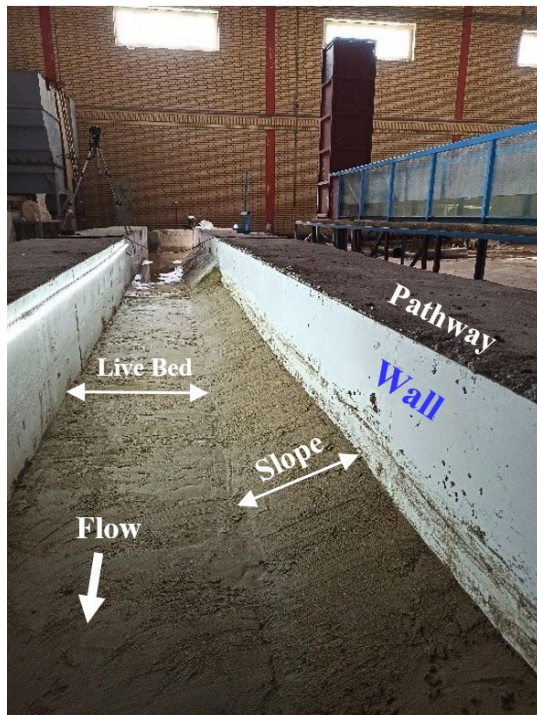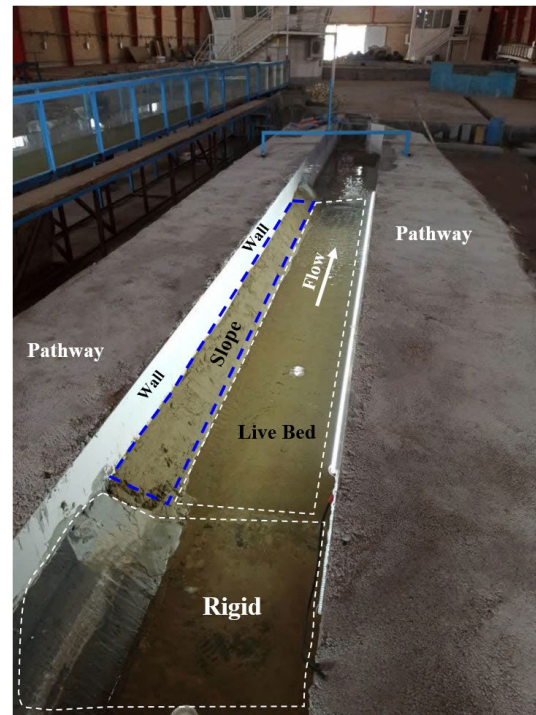| α	Q (Lit/s)	Fr_d
	8	0.2
	10	0.222
	12	0.23
20,25 and 30	14	0.24
	16	0.26
	18	0.27
	18.6	0.3

Fig 4 Laboratory Setup

After the conditions of flume, slope and current were defined, by leveling out the channel and providing the desired slope, the current was gradually released in the flume to obtain the desired flow. Subsequently, for 2h, the variations of the flume were inspected.

Based on the used scenarios and experiments, the conditions for incipient motion of the sediments were first examined. Since there was no intervening structure in the flow, no scouring, erosion and disruption of riverbanks were observed in 10 hours from the start of the experiments (untill reaching the sediment motion threshold ($U/U^*=1$)).

For all slopes, no changes occurred before sediment motion threshold ($U/U^*=1$). However, from Frd=0.2, the bed particles began to move ($U/U^*=1$). As such, the bank remained stable 10 hours from the start of the experiments. Up to $U/U^*=1$, the riverbank was stable and resisted destruction. From $U/U^*=1$ onwards, bank destruction and scouring occurred at the foot of the slope, until $U/U^*=1.75$.

3. Results and Discussion

This study shows the effects of side slope α at different ratios of threshold velocities U/U* on the time of failure Tf under the mobile bed conditions. Table 3 shows experiments in which riverbanks were destabilized and disrupted with time (after U/U*=1). Table 3 comprises 21 experiments. This table represents the time of failure T_f versus the depth of flow, with F and S standing for Fail and Stable, respectively.

Figure 5 shows the variations of the flow depth and bank slope versus the Froude number. According to the results, the bank conditions are stable on the left but unstable on the right side of the graph. The graph conditions, however, show the instability threshold. According to this figure, at a constant Froude number, while the slope decreases, the riverbank remains stable at greater flow depths. The figure also shows that the slope at $\alpha = 20$ degrees is in a better condition than the other two slopes ($\alpha = 30$ and 25) regarding the boundary between stable and unstable conditions, indicating that bank-flow interactions decrease as the slope decreases.

Figure 6 shows the steady state of riverbanks up to $U/U^*=1$. For all the three slopes, the conditions remained stable. Although slight changes and scouring were observed in flume bed sediments, the scouring was not strong enough to disrupt or destroy the riverbanks.

Figure 7 shows an experiment with the scouring of the river bed and the riverbank. In all the experiments, the scouring started from the bed and at the foot of the slope. The eroded area was gradually filled with slope sediments until the riverbank was destroyed. As a result, the slope became unstable and was reduced. After

U/U^*=1.7, the slope was removed and levelled out to the initial flume bed.

Table 3. Results summary

| Test	α	Fr_d	U/U^*	t_f(min)	h(m)	Fail/Stable
1		0.2	1.00	0	0.07	S
2		0.222	1.40	420	0.08	F
3		0.23	1.50	270	0.085	F
4	20	0.24	1.60	222	0.09	F
5		0.26	1.70	120	0.095	F
6		0.27	1.75	84	0.10	F
7		0.3	1.80	72	0.12	F
8		0.2	1.00	0	0.07	S
9		0.222	1.40	180	0.08	F
10		0.23	1.50	112	0.085	F
11	25	0.24	1.60	74	0.09	F
12		0.26	1.70	49	0.095	F
13		0.27	1.75	30	0.10	F
14		0.3	1.80	19	0.12	F
15		0.2	1.00	0	0.07	S
16		0.222	1.40	132	0.08	F
17		0.23	1.50	85	0.085	F
18	30	0.24	1.60	60	0.09	F
19		0.26	1.70	40	0.095	F
20		0.27	1.75	30	0.10	F
21		0.3	1.80	10	0.12	F
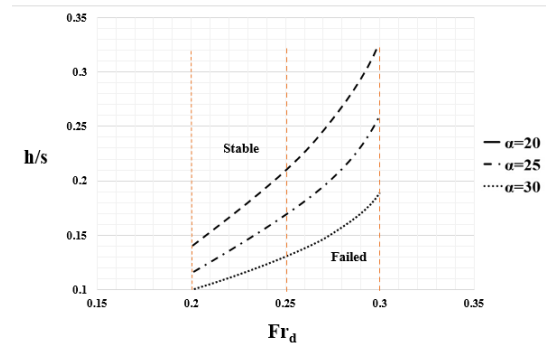
Fig 5. The lines mean the boundary between stable and unstable conditions

3.2. Effect of Fr_d on the Time of Failure T_f

This section investigates the effect of Fr_d on the time of failure T_f of the riverbank. In the diagram shown in Figure 8, the horizontal axis shows the value of the Froude number (Fr_d) and the vertical axis shows the time of failure (T_f).
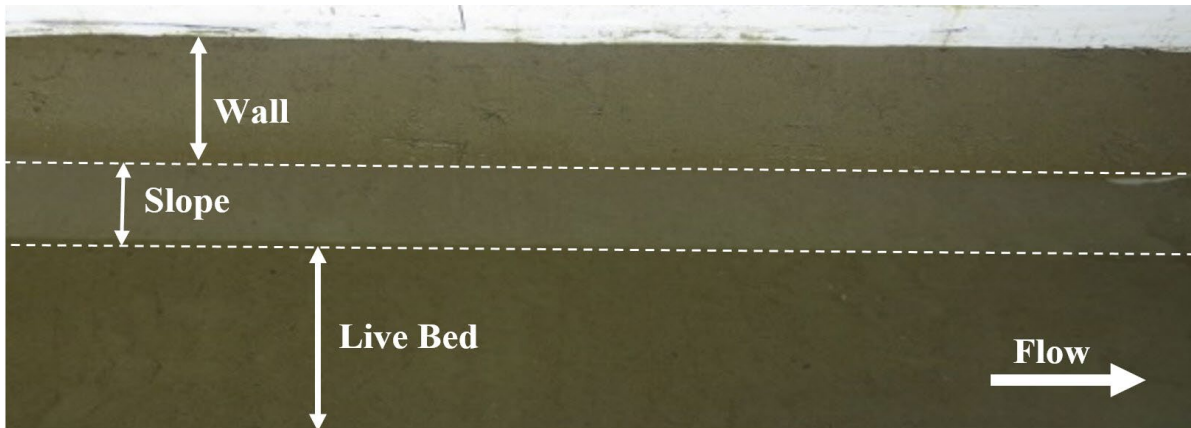

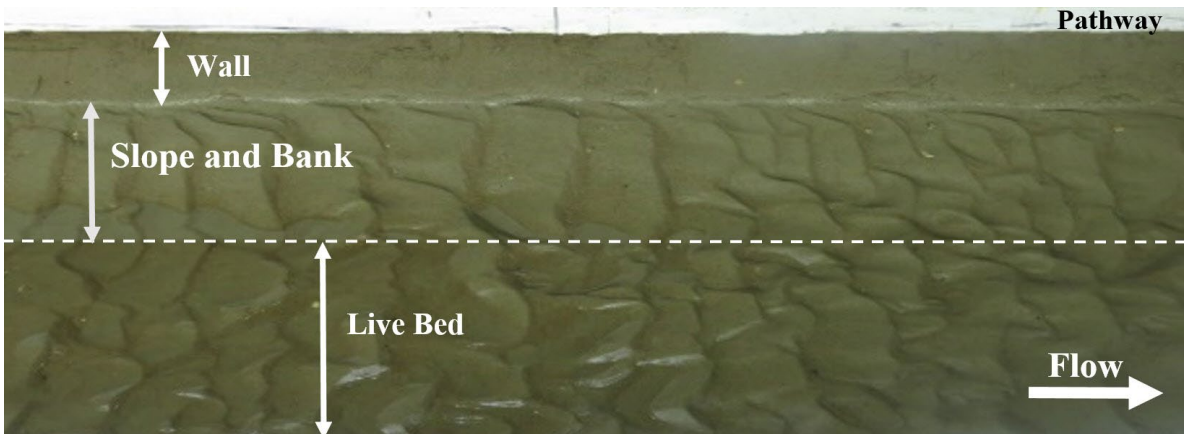**Fig. 6** Stable bank condition (U/U^*=1 & α=30)

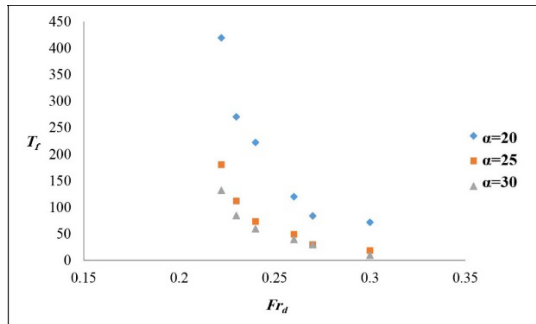**Fig. 7** Unstable bank condition (U/U^*=1.77 & α=30)

Fig. 8 Effect of Fr_d on T_f

As seen in Fig. 8, with the increase in Fr_d, the value of T_f decreases due to the increased distance from the motion threshold of the bed and wall particles. As the flow velocity increases, the instability increases and riverbank destruction occurs in a shorter time. The failure time Tf indicates the time of the beginning of failure and collapse of the riverbank. As the value of T_f increases, the riverbank becomes more stable against flow hydraulic conditions.

At Froude number 0.2, all the three slopes were stable, and the riverbank was not destroyed until 120 minutes from the beginning of the experiments. As is seen, the riverbank with a slope of 20 degrees is destroyed after the other two slopes (25 and 30 degrees). At Froude numbers larger than 0.2, all the slopes became unstable. However, the instability occurred in a longer time for the 20° slope, compared to the other two slopes.

4. Conclusion

In this research, 21 experiments were conducted in the Sediment Research Center of Khuzestan Water and Power Organization on a river model with mobile bed conditions. The study aimed to show the effects of the slope and the flow on riverbank stability under the mobile bed conditions. As opposed to the solid bed conditions in the literature, in the present study, the bed conditions as well as the scouring and destruction processes are assumed to be mobile, various and varied, as in the real rivers. The conditions were stable up to a certain limit (Fr_d=0.21 and U/U^*=1), and no changes or destruction occurred with time (up to 10 hours). After this limit, the foot of the slope started to erode, and riverbank sediments slowly entered the erosion hole and washed downstream. Subsequently, the side slope started to overturn and collapse. At more than U/U^*=1.70, the side slope completely removed and became level

with the river bed. According to the results of the study, the riverbank with a slope of 20 degrees is destroyed after the other two slopes (25 and 30 degrees). At Froude numbers over 0.2, the slopes were all unstable, although it took a longer time for the 20° slope, compared to the other two slopes, to become unstable. As the value of Fr_d increased, the failure time T_f decreased, which can be explained by distancing away from the motion threshold of the bed and the wall particles. As the flow rate increased, the bank became more unstable and destroyerd in a shorter time. In live bed conditions, compared to clear water conditions, the local scouring and distruction of structres are faster, although the scouring speed might not be maximum.

5. Notation

D_{50}	Sediment granulation (m)
Fr_d	Densimetric Froude number ratio
g	Acceleration of gravity (ms^{-2})
h	Water depth (m)
Q	Discharge (lits^{-1})
S	Longitudinal slope (m^{-1})
S_B	Specific gravity of blocks Ratio
T_f	Fail time (s)
U	Velocity (ms^{-1})
U^*	Incipient motion velocity (ms^{-1})
W	Channel width (m)
Greek letters	
α	Bank slope (m^{-1})
ρ	Density (kgm^{-3})
ρ_s	Saturated sediment particle Density (kgm^{-3})
μ	Dynamic Viscosity (kgm^{-1}s^{-1})
v	Kinematic Viscosity (m^{2}s^{-1})

6. References

Azinfar, H. & Kells, J. (2018). Backwater prediction due to the blockage caused by a single, submerged spur dike in an open channel. *Journal of Hydraulic Engineering*, *134*(8), 1153-1157 .

Bakhtiari, M., Kashefipour, S., Ghomeshi, M. & Zahiri, J. (2012). Effect of geometric parameters of spur dike and depth-placed riprap on its failure threshold in a 90 flume bend. *Ecol. Environ. Conserv*, *4*, 479-484 .

Cancienne, R.M., Fox, G.A. & Simon, A. (2019). Influence of seepage undercutting on the stability of root-reinforced streambanks.

Earth Surface Processes and Landforms, *33*(11), 1769-1786.

Chu-Agor, M., Wilson, G. & Fox, G.A. (2008). Numerical modeling of bank instability by seepage erosion undercutting of layered streambanks. *Journal of Hydrologic Engineering*, *13*(12), 1133-1145 .

Etminan, Z., Rostami, M. & Nosrati, K. (2020). Evaluation of River Bank Stability against Erosion and Management Practices of Taleghan River Bank Using LIN Method. *Iranian journal of Ecohydrology*, *7*(1), 111-119 .

Fox, G., Chu-Agor, M. & Wilson, G. (2018). Seepage erosion: A significant mechanism of stream bank failure. Paper presented at the World Environmental and Water Resources Congress 2007: Restoring our natural habitat, https://doi.org/10.1061/40927(243)350.

Froehlich, D. (2013). Sizing loose rock riprap to protect stream banks. *River Research and Applications*, *29*(2), 219-235.

Grace, J.L., Calhoun, C.C. & Brown, D.N. (1973). Drainage and erosion control facilities: Field performance investigation: US Army Engineering Waterways Experiment Station, Hydraulics Laboratory.

Hackney, C.R., Darby, S.E., Parsons, D.R., Leyland, J., Best, J. L., Aalto, R., Nicholas, A.P, & Houseago, R.C. (2020). River bank instability from unsustainable sand mining in the lower Mekong River. *Nature Sustainability*, *3*(3), 217-225.

Jafarnejad, M., Franca, M.J., Pfister, M. & Schleiss, A.J. (2018). Effect of a second layer on the time to failure of compressed riprap as mountain riverbank protection. *Journal of*

Hydraulic Research, *57*(4), 573-578, https://doi.org/10.1080/00221686.2018.1494048.

Jafarnejad, M., Franca, M. J., Pfister, M., & Schleiss, A. J. (2019). Design of riverbank riprap using large, individually placed blocks. *Journal of Hydraulic Engineering*, *145*(12), 04019042, https://doi.org/10.1061/(ASCE)HY.1943-7900.0001641.

Krzeminska, D., Kerkhof, T., Skaalsveen, K. & Stolte, J. (2019). Effect of riparian vegetation on stream bank stability in small agricultural catchments. *Catena*, *172*, 87-96 .

Li, B., Li, T., Xu, N., Dai, F., Chen, W. & Tan, Y. (2018). Stability assessment of the left bank slope of the Baihetan Hydropower Station, Southwest China. *International Journal of Rock Mechanics and Mining Sciences*, *104*, 34-44 .

Ravindra, G.H., Gronz, O., Dost, J.B. & Sigtryggsdóttir, F. G. (2020). Description of failure mechanism in placed riprap on steep slope with unsupported toe using smartstone probes. *Engineering Structures*, *221*, 111038, https://doi.org/10.1016/j.engstruct.2020.111038.

Schnellmann, R., Busslinger, M., Schneider, H. R. & Rahardjo, H. (2019). Effect of rising water table in an unsaturated slope. *Engineering Geology*, *114*(1-2), 71-83 .

Thorne, C.R. & Lewin, J. (2020). Bank processes, bed material movement and planform development in a meandering river, In: Adjustments of the fluvial system, Rhodes, D.D., Williams, G.P., eds., 117-137, Routledge.

Wilson, G., Periketi, R. & Cullum, R. (2017). Sediment transport model for seepage erosion of streambank sediment. *Journal of Hydrologic Engineering*, *11*(6), 603-611 .